EBioMedicine 73 (2021) 103672

Contents lists available at ScienceDirect

EBioMedicine

journal homepage: www.elsevier.com/locate/ebiom

α-Ketoglutarate Inhibits Thrombosis and Inflammation by Prolyl Hydroxylase-2 Mediated Inactivation of Phospho-Akt

Nishith M Shrimali[1], Sakshi Agarwal[1], Simrandeep Kaur[1], Sulagna Bhattacharya[1], Sankar Bhattacharyya[2], Josef T Prchal[3], Prasenjit Guchhait[1,*]

[1] Regional Centre for Biotechnology; National Capital Region Biotech Science Cluster, Faridabad, India
[2] Translational Health Science Technology Institute; National Capital Region Biotech Science Cluster, Faridabad, India
[3] Department of Medicine, University of Utah School of Medicine & Huntsman Cancer Center and George E. Whalen Veteran's Administration Medical Center, Salt Lake City, UT, USA

ARTICLE INFO

Article History:
Received 10 August 2021
Revised 15 October 2021
Accepted 20 October 2021
Available online xxx

Keywords:
αKG
PHD2
Akt
thrombosis
inflammation
SARS-CoV-2

ABSTRACT

Background: Phospho-Akt1 (pAkt1) undergoes prolyl hydroxylation at Pro125 and Pro313 by the prolyl hydroxylase-2 (PHD2) in a reaction decarboxylating α-ketoglutarate (αKG). We investigated whether the αKG supplementation could inhibit Akt-mediated activation of platelets and monocytes, in vitro as well as in vivo, by augmenting PHD2 activity.

Methods: We treated platelets or monocytes isolated from healthy individuals with αKG in presence of agonists in vitro and assessed the signalling molecules including pAkt1. We supplemented mice with dietary αKG and estimated the functional responses of platelets and monocytes ex vivo. Further, we investigated the impact of dietary αKG on inflammation and thrombosis in lungs of mice either treated with thrombosis-inducing agent carrageenan or infected with SARS-CoV-2.

Findings: Octyl αKG supplementation to platelets promoted PHD2 activity through elevated intracellular αKG to succinate ratio, and reduced aggregation in vitro by suppressing pAkt1(Thr308). Augmented PHD2 activity was confirmed by increased hydroxylated-proline and enhanced binding of PHD2 to pAkt in αKG-treated platelets. Contrastingly, inhibitors of PHD2 significantly increased pAkt1 in platelets. Octyl-αKG followed similar mechanism in monocytes to inhibit cytokine secretion in vitro. Our data also describe a suppressed pAkt1 and reduced activation of platelets and leukocytes ex vivo from mice supplemented with dietary αKG, unaccompanied by alteration in their number. Dietary αKG significantly reduced clot formation and leukocyte accumulation in various organs including lungs of mice treated with thrombosis-inducing agent carrageenan. Importantly, in SARS-CoV-2 infected hamsters, we observed a significant rescue effect of dietary αKG on inflamed lungs with significantly reduced leukocyte accumulation, clot formation and viral load alongside down-modulation of pAkt in the lung of the infected animals.

Interpretation: Our study suggests that dietary αKG supplementation prevents Akt-driven maladies such as thrombosis and inflammation and rescues pathology of COVID19-infected lungs.

Funding: Study was funded by the Department of Biotechnology (DBT), Govt. of India (grants: BT/PR22881 and BT/PR22985); and the Science and Engineering Research Board, Govt. of India (CRG/000092).

1. Introduction

The serine-threonine kinase Akt, also known as protein kinase B (PKB), contributes to a broad range of cellular functions including cell survival, proliferation, gene expression and migration of cells of most lineages. Akt plays a central role in both physiological and pathological signalling mechanisms. Upon exposure to stimuli, Akt is recruited to the cell membrane by phosphoinositide 3-kinase (PI3K), where it is phosphorylated by membrane associated 3-phosphoinositide-dependent kinase-1 (PDK1), leading to its activation. Among the three identified isoforms, Akt1 is widely expressed in most human and mouse cells [1-5]. The crucial role of PI3K-Akt signalling has been elucidated in platelet activation and functional responses including aggregation, adhesion and thrombus formation [1-7]. Akt1$^{-/-}$ mice displayed an increased bleeding time and their platelets showed decreased response to agonists ex vivo [3]. Both Akt1 and Akt2 are reported to facilitate GP2b3a binding to soluble fibrinogen and thus platelet aggregation at low concentration of agonist [2,3]. Akt2 and Akt3 play important role in granule secretion and aggregation in

* Correspondence to Prasenjit Guchhait
E-mail address: prasenjit@rcb.res.in (P. Guchhait).

https://doi.org/10.1016/j.ebiom.2021.103672

Research in context

Evidence before this study

It has been reported that prolyl hydroxylase-2 (PHD2) can inactivate phosphorylated Akt (pAkt). In von-Hippel-Lindau (VHL)-deficient/suppressed cells and under hypoxic microenvironment, accumulation of pAkt is likely to promote tumor growth. The inhibition of pAkt partially reverses this tumorigenic effect. Studies, including the above work, have described that PHD2 catalyses proline hydroxylation of its substrates with concomitant conversion of O2 and α-ketoglutarate (αKG) to CO2 and succinate, respectively. Succinate can inhibit PHD2 by competing with αKG. Therefore, an elevated intracellular ratio of αKG to succinate may be employed as a marker of PHD2 activity.

Added value of this study

Our study for the first time describes the regulatory role of the PHD2-pAkt axis in platelet and monocyte functional responses under normoxia. We report an inactivating impact of αKG mediated augmentation of PHD2 activity on phosphorylated Akt1 (pAkt1). An elevated ratio of αKG to succinate in αKG-supplemented platelets and monocytes significantly augmented PHD2 activity and in turn downmodulated pAkt1. Dietary αKG significantly reduced clot formation and leukocyte accumulation in various organs, including lungs, of mice treated with thrombosis-inducing agent carrageenan. Importantly, in SARS-CoV-2 infected hamsters, we observed a significant rescue effect of dietary αKG on inflamed lungs with significantly reduced leukocyte accumulation, clot formation, and viral load alongside downmodulation of pAkt in lungs of the infected animals.

Implications of all the available evidence

This study proposes a safe supplement of dietary aKG to curtail Akt-driven thrombosis and inflammation in various pathologies, including the inflamed lungs of COVID-19 patients. The study also highlights aKG-PHD2-pAkt axis as a potential target for better pulmonary management in such diseases.

response to thrombin and TxA2 in vitro and also in arterial thrombosis in vivo [3,5]. Therefore, several studies have used Akt inhibitors like SH-6, triciribine and Akti-X in an attempt to abrogate platelet aggregation, clot formation and granule secretion in vitro as well as in vivo [4, 8-9].

The crucial involvement of PI3K-Akt pathway in regulation of immune cell functions in a broad range of inflammatory diseases such as rheumatoid arthritis, multiple sclerosis, asthma, chronic obstructive pulmonary disease, psoriasis and atherosclerosis has been documented [10-15]. Pathological signalling of Akt is also well reported in progression of cancer [16]. Activation of PI3K-Akt pathway plays an important role in host immune response to infections including SARS-CoV-2, [17-18] SARS-CoV, [19] Dengue and Japanese Encephalitis [20] viruses, wherein Akt signalling is pivotal for the virus entry and replication in host cells. Therefore, Akt is a potential therapeutic target in various disease conditions [21]. The PI3K-Akt inhibitor wortmannin has been used to alleviate severity of inflammation and improve survival rate in rats with induced severe acute pancreatitis. Akt1$^{-/-}$ mice had reduced carrageenan-induced paw oedema and related inflammation alongside a significant decrease in neutrophil and monocyte infiltration [22]. Studies using inhibitors such as Akti-8 and Akt-siRNA support the crucial regulatory role of Akt in inflammatory response of monocytes and macrophages in vitro and in vivo [23-24].

It has been reported that phosphorylated Akt1 (pAkt1) is hydroxylated by an oxygen-dependent enzyme, prolyl hydroxylase 2 (PHD2). The pAkt1 undergoes prolyl hydroxylation at Pro125 and Pro313 by PHD2 in a reaction decarboxylating α-ketoglutarate (αKG). This promotes von Hippel−Lindau protein (pVHL) binding to the PHD2 hydroxylated site. pVHL then interacts with protein phosphatase 2A (PP2A), which dephosphorylates Thr308 and to a lesser extent Ser473, resulting in Akt1 inactivation [25].

In this study, we describe a heretofore unreported role of PHD2 in regulation of platelet and monocyte functions by inactivating pAkt1. Supplementation with dietary αKG, a metabolite of TCA cycle and a cofactor of PHD2, appears to be a potent suppressor of pAkt, significantly reducing thrombotic and inflammatory events in mice treated with thrombosis-inducing agent carrageenan [26]. Reports suggest that SARS-CoV-2 directly activates platelets [27,28] and symptoms like thrombosis and inflammation are common in severe forms of COVID-19 [29]. We have tested the rescue effect of dietary αKG on lung inflammation in SARS-CoV-2 infected golden hamsters. The hamster model is well-studied for SARS-CoV-2 infection. Studies have reported that SARS-CoV-2 infection induces significant inflammation of the bronchial epithelial cells and lungs in hamsters [30]. Here, we show that SARS-CoV-2 increases phosphorylation of Akt1 (Thr308) [17], a known target of PHD2, in infected cells. We describe that dietary αKG significantly reduces clot formation, inflammation and viral load in conjunction with down-modulation of pAkt in lungs of SARS-CoV-2 infected golden hamsters.

2. Methods

2.1. Ethics

Human ethics approval was obtained from the Institutional Ethics Committee (IEC) for human research of Regional Centre for Biotechnology (RCB; ref no. RCB-IEC-H-08) to recruit healthy volunteers. Written informed consent was received from all participants.

Animal ethics approval was obtained from the Institutional Animal Ethics Committee (IAEC) of RCB (ref. no. RCB/ IAEC/2020/077) and experiments using BALB/c mouse strain (RRID: IMSR_JAX_000651) were conducted within the guidelines of IAEC in the Small Animal Facility (SAF) of our institute. Animal ethics approval for SARS-CoV-2 work was obtained from the IAEC (ref. no. RCB/IAEC/2020/069) and Institutional Biosafety Committee (IBSC; ref. no. RCB/IBSC/20-21/221) of RCB and experiments using Syrian golden hamster (available form ICMR-National Institute of Nutrition, Hyderabad, India) were conducted within the guidelines of IAEC in the BSL3 facility of our institute.

2.2. Platelet and monocyte isolation

Whole blood was collected form healthy individuals in sodium citrate or ACD anticoagulant. Platelets and monocytes were isolated from whole blood and used for in vitro experiments. Volunteers were recruited on the basis of inclusion criteria: 1) healthy, 2) not taking any anti-platelet or anti-inflammatory drugs, 3) no major illness or chronic disease, and 4) no microbial infections within a month of recruitment. Number of healthy individuals recruited for each experiment has been mentioned in respective Figure legends. A written informed consent was received from all participants. 16 ml of whole blood was collected from healthy volunteers by venepuncture in vacutainers containing anti-coagulant sodium citrate or acid-citrate dextrose (ACD). Platelet rich plasma (PRP) was separated by centrifugation at 44 g for 15 min. Sodium citrate containing PRP was used for aggregation and activation studies. PRP in ACD was used for isolating washed platelets for further studies as described in our previous work [31].

Peripheral blood mononuclear cells (PBMCs) were isolated using Ficoll Hypaque (GE Healthcare, Freiburg, Germany) density gradient centrifugation as described [32]. PBMCs were washed twice with phosphate buffered saline (PBS), pH 7.4 and seeded in cell culture-treated plates (Corning, NY, USA) in RPMI-1640 medium (Sigma Aldrich, USA) supplemented with 10% (v/v) foetal bovine serum (Gibco Invitrogen, San Diego, CA), 100 U/mL penicillin and 100 μg/mL streptomycin for 2 hrs at 37°C in a humidified atmosphere with 5% CO^2, to allow monocytes to adhere to the plate. After 2 hrs, supernatant containing non-adherent cells were removed and adhered monocytes were used for further treatments described hereafter.

2.3. Platelet activation and aggregation assays

Human PRP diluted (1:1) in Tyrod's buffer pH 7.2 was used for following assays. Diluted PRP was pre-treated with octyl α-ketoglutarate (Sigma Aldrich, USA) or inhibitors to PHD2 such as dimethyl ketoglutarate (DKG, Sigma Aldrich) or ethyl-3-4-dihydroxybenzoic acid (DHB, TCI America, Portland) and incubated with collagen (10 μg/ml) or ADP (2 μM, both from the Bio/Data Corporation, USA) 10 minutes. Platelets were labelled with P-selectin (PE Cy5), PAC-1 (FITC) and Annexin-V (FITC) antibodies (BD bioscience) for 15 min at 37°C and fixed in 1% paraformaldehyde. 20,000 events were acquired using flow cytometry (BD FACS Verse). The acquired data was analysed using the Flowjo software (Tree Star, USA), as described [31]. Supplementary Table S1 lists the details of antibodies that have been used in immunoblot, immunoprecipitation and flow cytometry based experiments.

Platelet aggregation was performed using PAP8 aggregometer (Bio/Data Corporation, USA). PRP was pre-treated with αKG or DKG and incubated with collagen (20 μg/ml) or ADP (5 μM) and aggregation percentage was measured.

2.4. Platelet thrombus formation assay

Platelet thrombus formation assay was performed by perfusing whole blood (collected in citrate-anticoagulant from healthy individuals) in the Petri plate immobilized with collagen. Whole blood was preincubated for 5 min with either αKG or DKG or both before perfusion on collagen coated surface. A syringe pump (Harvard Apparatus Inc., USA) was connected to the outlet port that drew blood through the chamber at arterial shear stress of 25 dyne/cm^2. The flow chamber was mounted onto a Nikon Eclipse Ti-E inverted stage microscope (Nikon, Japan) equipped with a high-speed digital camera. Movies were recorded at magnification 40X and analysed using NIS-Elements version 4.2 software as described in our previous study [33].

2.5. Platelet microparticle measurement

PRP was pre-treated with/without αKG and incubated with collagen for 10 min. Platelet-free plasma was obtained by 2 sequential centrifugations: PRP at 1500 g for 7 min followed by platelet-poor plasma (PPP) at 1500 g for 15 min. Platelet-derived microparticles (MPs) were measured using flow cytometry after labelling with anti-CD41 PE antibody as mentioned [31].

2.6. Monocyte activation

Primary monocytes and monocytic cell line were pre-treated with 1mM octyl α-ketoglutarate (Sigma Aldrich, USA) for 2 hrs and 4 hrs respectively followed by replacement with fresh media. Cells were treated with either S1P (1 μM) or LPS (500 ng/ml). Treated cell supernatant was used for assessing cytokines using the cytometric bead array (CBA). Protein lysate prepared from cell pellet was used for western blotting of signalling molecules.

2.7.CBA. for quantifying cytokines

Cytokines such as TNF-α, IL-1β, IL-6 and IL-10 were measured from human primary monocytes culture supernatant or mice plasma of different treatments as described in Results using CBA and analysed by FCAP array software (BD Biosciences, San Jose, CA,USA).

2.8. Generation of HIF-1α depleted monocyte cell line

HIF-1α protein expression was depleted in human U937 cell line (RRID:CVCL_0007) using shRNA targeting HIF-1α (TCRN0000010819, Sigma Aldrich, USA) using a liposome mediated delivery (Life Technologies, Thermo Fisher Scientific, USA). The original cell line is validated and was also Mycoplasma contamination free.

2.9. Generation of PHD2 depleted monocyte cell line

PHD2 was depleted in human U937 cell line using shRNA targeting *EGLN1* as described [34]. The original cell line is validated and was also Mycoplasma contamination free.

2.10. Dietary αKG supplementation to mice and hamsters

Male BALB/c mice aged 5-7 weeks or Syrian golden hamsters of 8 weeks were supplemented with 1% of dietary α-ketoglutarate (SRL, Mumbai, India) in drinking water for 24 or 48 hrs (to mice), or for 6 days (to hamsters) as described in schematic Fig. 4, 5 and 6. The blood cell counts and other assays were performed.

2.11. Mice platelet aggregation

PRP was collected from control and αKG-treated mice. The sample size calculation was performed after doing a pilot study with 4 BALB/c mice per group. Based on the outcome of this pilot study, we calculated number of mice per group at a confidence interval of 95% and power of 80% to get a p-value less than 0.01 (http://www.lasec.cuhk.edu.hk/sample-size-calculation.html). The predicted number of mice to be kept in each group was calculated, n=6. PRP was and diluted with PBS (1:1 vol) and processed for centrifugation at 90 g using brake-free deceleration on a swinging bucket rotor for 10 min. Platelets counts were adjusted to 2.5×10^8/ml and platelet aggregation was evaluated using PAP8 aggregometer. Collagen (7.5 μg/ml) or ADP (5 μM) was used as aggregation agonist.

2.12.Carrageenan. treatment to mice and measuring thrombosis and cellularity scores

BALB/c mice were used to develop carrageenan-induced thrombosis model [35]. The sample size calculation was performed after doing a pilot study with 4 BALB/c mice per group. Based on the outcome of this pilot study, we calculated number of mice per group at a confidence interval of 95% and power of 80% to get a p-value less than 0.01 (http://www.lasec.cuhk.edu.hk/sample-size-calculation.html). The predicted number of mice to be kept in each group was calculated, n=7. Mice were injected with 100 μl of 10 mg/ml κ-carrageenan (Sigma Aldrich, USA) prepared in normal saline in intraperitoneal cavity. αKG was supplemented via drinking water to these mice. After 48 hrs of carrageenan treatment, length of thrombus covered tail was measured and percentage tail thrombosis was calculated by length of thrombus covered tail/total length of tail$\times$100.

Thrombosis score was measured in mice lungs and livers. Lungs and liver samples were fixed in 4% formalin and paraffin embedded. 2.5 μm thick sections were prepared and stained with Haematoxylin and Eosin (H&E) and Masson's trichrome (MT). Slides were observed under Nikon Eclipse Ti-E inverted stage microscope (Nikon, Japan)

and images were acquired at 20 X to observe thrombi and at 40X to observe leukocyte accumulation. Thrombosis scoring was calculated using ImageJ software. Thrombi were selected using freehand selection tool in MT-stained slides. Percentage area covered was calculated as percentage of freehand selected area covering the total area. The lung sections were used for immunostaining using platelet marker CD42c antibody. The leukocyte accumulation was assessed as a marker of inflammation in the above lung section using percentage cellularity. Cellularity score was calculated using ImageJ software. Images were converted to RGB stack and from that all nuclei were selected based on the intensity of colour and size from H&E-stained slides. Percentage area covered by nucleated cells was calculated by measuring nuclear area as a percentage of the total tissue section area.

Carrageenan-induced peritoneal inflammation was measured in mice using a modified protocol as described [35,36]. BALB/c mice received carrageenan (10 mg/ml) or saline intraperitoneally. At 3hrs and 6hrs, the animals were anaesthetized and peritoneal exudates were harvested in 3 ml of PBS. Different immune cell populations in peritoneal lavage were analysed and cell types were identified by flow cytometry using CD45.2, CD11b, CD11c, Ly6G, Ly6C, and CD41 expression [32,33]. In another set of a similar experiment, BALB/c mice were injected with carrageenan. At 3 and 6 hrs, peritoneal inflammation was visualised using bioluminescence-based imaging of MPO activity by injecting luminol (i.p. 20 mg/100 g body weight) (Sigma Aldrich) 6 min prior to imaging using an in-vivo imaging system (IVIS; Perkin Elmer, Waltham, MA, USA) as described in our work [32].

2.13. SARS-CoV-2 infection to Syrian golden hamsters

The hamster model of SARS-CoV-2 infection has been well established [30]. Male hamsters of 8 weeks old were infected with SARS-CoV-2 (isolate USA-WA-1/2020 from World Reference Center for Emerging Viruses and Arboviruses, from UTMB, Texas, USA), via nasal route inoculation using 1×10^6 plaque-forming units (PFU) as described [30].

1% dietary αKG was administered via drinking water and 400μl of 10% αKG was given through oral gavage on day 3 through day 5. The sample size calculation was performed after doing a pilot study with 3 Male golden hamsters per group. Based on the outcome of this pilot study, we calculated number of hamsters per group at a confidence interval of 95% and power of 80% to get a p-value less than 0.01 (http://www.lasec.cuhk.edu.hk/sample-size-calculation.html). The predicted number of hamsters to be kept in each group was calculated, n=5. During this phase, hamsters were symptomatic and were not drinking sufficient (male hamster of 100 gm B wt. drinks normally 5 ml per day) water. The schematic protocol of infection and therapy is described in Fig. 6. At day-6, animals were sacrificed and lungs and liver samples were harvested, fixed in 4% formalin, paraffin embedded and processed for H&E and MT staining. The thrombosis and inflammation scores were measured as described above. The lung sections were used for immunohistochemistry staining for pAkt (Cell Signalling Tech, USA) Body weight was recorded on alternate days. The lung sections were used for measuring viral genome using RT-PCR.

2.14. SARS-CoV-2 infection to cell line

Human liver cell line Huh7 (RRID:CVCL_0336) seeded ($6x10^4$ cells/well) and pre-treated with 1mM octyl αKG for 2 hrs and infected with 0.1 MOI of SARS-CoV-2 for 24 hrs in BSL3 facility. The cells pellet was lysed and fixed for using estimation of pAkt1 using Western blotting. The original cell line is validated and was also Mycoplasma contamination free.

2.15. RT-PCR detection of viral genome

Lung tissue sample from hamsters was homogenized in Trizol reagent (MRC, UK) using a hand-held tissue-homogenizer and the total RNA extracted as per manufacturer's protocol. 1 μg total RNA was reverse-transcribed using Superscript-III reverse-transcriptase (Invitrogen, USA) as per manufacturer's protocol, using random hexamers (Sigma Aldrich, USA). The cDNA was diluted in nuclease-free water (Promega, USA) and used for real-time PCR with either SARS-CoV-2 or GAPDH specific primers, using 2x SYBR-green mix (Takara Bio, Clontech, USA) in an Applied Biosystems® QuantStudio™ 6 Flex Real-Time PCR System. The oligonucleotides used were SARS-F (5′-CAATGGTTTAACAGGCACAGG-3′) and SARS-R (5′-CTCAAGTGTCTGTGGATCACG-3′) for SARS-CoV-2, and G3PDH-F (5′-GACATCAAGAAGGTGGTGAAGCA-3′) and G3PDH-R (5′-CATCAAAGGTGGAAGAGTGGGA-3′). The Ct value corresponding the viral RNA was normalised to that of G3PDH transcript. The relative level of SARS-CoV-2 RNA in mock-infected samples was arbitrarily taken as 1 and that of infected samples expressed as fold-enrichment (FE). The FE value for each infected sample was transformed to their logarithmic value to the base of 10 and plotted.

The viral genome was measured in Huh7 cell line treated with SARS-CoV-2 using RT-PCR as described above. The Ct value corresponding the viral RNA was normalised to that of RNAse P (RP) transcript. The oligonucleotides used were RP-F (5′-AGATTTGGACCTGCGAGCG-3′) and RP-R (5′-GAGCGGCTGTCTCCACAAGT-3′).

2.16. Immunoprecipitation

PHD2 was immunoprecipitated from platelet lysate using protein G Sepharose beads and anti-PHD2 antibody (Cell Signalling Tech, USA). Similarly, phosphorylated Akt (pAkt) was immunoprecipitated using protein A Sepharose beads and anti-pAkt antibody (Cell Signalling Tech, USA). Briefly, washed platelets isolated from whole blood of healthy volunteer and lysed in lysis buffer (25 mM Tris, 150 mM sodium chloride, 1 mM EDTA, 1% NP-40, 50 mM sodium fluoride and 3% Glycerol) with protease and phosphatase inhibitor. Lysate was pre-cleared with protein A or G Sepharose beads and then added to antibody coated beds and incubated overnight. Beads were removed, washed with lysis buffer and collected protein sample was processed for western blotting.

2.17.Western. blotting

The whole cell (platelets or primary monocyte or monocytic cell line) lysate was prepared using RIPA lysis buffer and protease-phosphatase inhibitor (Thermo Scientific Life Tech, USA). SDS-PAGE gel was followed by immunoblotting using primary antibodies against pAkt(Ser4730, Akt, pAkt1(Thr 308), Akt1, HIF-1α, HIF-2α, β-Actin (Cell Signalling, USA) and α-tubulin (Thermo Fisher Scientific, USA) as described in detail in our previous work [31]. The detailed information of antibodies is described in Table S1.

2.18. Estimation of metabolites

Steady-state level of α-ketoglutarate, lactate, fumarate, pyruvate and succinate was estimated in plasma, PBMC-granulocytes (10^5) and platelets (10^5) of mice or human samples from different treatments as per manufacture protocol (Sigma Aldrich, USA catalogue no. MAK054, MAK064, MAK060, MAK071, MAK335 respectively).

2.19. Sphingosine-1-Phosphate measurement

αKG treated and control mice platelets were stimulated with collagen (10 μg/ml) in vitro and supernatant was collected and used to

estimate Sphingosine-1-phosphate (S1P) level as per manufacturer's protocol [Cloud clone corp. (CEG031Ge)]. Similarly, human platelets were treated with αKG and collagen (5 μg/ml) and supernatant were used to estimate S1P level. The detailed information of reagents used in this study is described in Table S2.

2.20. Statistical Analysis

Data from at least three experiments are presented as mean ± SEM (standard error of the mean). Statistical differences among experimental sets with normally distributed data were analysed by using either unpaired t test, or one-way or two-way ANOVA followed by Bonferroni's correction for multiple comparison. Kruskal Wallis test followed by Dunn's multiple comparison post-test was used for non-normally distributed data. D'Agostino-Pearson Test was used to check for normal distribution of data. Graph Pad Prism version 8.0 software was used for data analysis and *P*-values <0.05 were considered statistically significant.

3. Role of funding source

This study is supported by BT/PR22881 and BT/PR22985 from the Department of Biotechnology (DBT), Govt. of India; and CRG/000092 from the Science and Engineering Research Board, Govt. of India to PG. The funder had no role in study design, data collection, data analysis, interpretation, or writing the manuscript.

4. Results

4.1. Platelet activation directly relates to phosphorylated Akt1 but inversely with prolyl-hydroxylase activity of PHD2

We searched for the presence of all 3 isoforms PHD1, PHD2 and PHD3 in platelets (Fig. 1a). A recent report has shown that PHD2 hydroxylates the proline residues of phosphorylated Akt1(Thr308) [pAkt1(Thr308)] eventually leading to inactivation [25]. Therefore, we measured phosphorylation status of Akt1 and PHD2 activity in agonist-activated platelets in normoxia. As expected, the phosphorylation of Akt(Ser473) and Akt1(Thr308) increased in tandem with higher concentrations of agonists, collagen (*P<0.05, **P<0.01, ****P<0.0001; Fig. 1b-d) and ADP (**P<0.01, ****P<0.0001; Fig. S1a), indicating attenuated activity of PHD2. Also, we measured expression of other known substrates of PHD2 such as HIF1α and HIF2α in agonist-activated platelets. The increased expression of HIF1α and HIF2α (**P<0.01, ***P<0.001, ****P<0.0001; Fig. 1b) suggested a lower activity of PHD2 in activated platelets. This suggested that the enzymatic activity of PHD2 remains below the threshold level to inactivate pAkt.. We then tested whether agonist or other chemical induced alteration in prolyl-hydroxylase activity of PHD2 can in turn alter the activation status of pAkt in platelet.

4.2. Supplementation of octyl αKG inhibits Akt1 phosphorylation by augmenting PHD2 activity

To alter the enzymatic activity of PHD2, we used α-ketoglutarate (αKG, a cofactor of PHD2) and dimethyl ketoglutarate (DKG, an inhibitor to PHD2). Octyl αKG (a membrane-permeating form) supplementation significantly decreased the collagen-induced phosphorylation of Akt1 (Thr308) and Akt(Ser473) (*P<0.05, ***P<0.001, ****P<0.0001; Fig. 1e-g), and also degraded HIF1α and HIF2α (*P<0.05, **P<0.01; Fig. 1e-g) in platelets under normoxia. Interaction of pAkt1 with PHD2 was confirmed by immunoprecipitation of PHD2 followed by immunoblotting for pAkt1(Thr308). In presence of αKG, enzymatically active PHD2 displayed increased binding to pAkt1(Thr308) (****P<0.0001; Fig. 1h), resulting into the inactivation of pAkt1 in collagen-activated platelets. In order to evaluate the prolyl-hydroxylation activity of PHD2 on pAkt, immunoprecipitation was performed using Akt(Ser473) antibody and immunoblotted for hydroxylated proline. Increased levels of pAkt-bound hydroxy proline (*P<0.05; Fig. 1h), suggested an elevated hydroxylation of proline on pAkt in platelets in presence of αKG. On the other hand, the PHD2 inhibitor DKG favoured the Akt phosphorylation (Fig. 1e-g). Other known inhibitor of PHD2, ethyl-3-4-dihydroxybenzoic acid (DHB), also elevated phosphorylation of Akt1(Thr308) and Akt (Ser473) (*P<0.05, **P<0.01; Fig. S1b). Although, αKG and DKG altered the enzymatic function of the PHD2 to regulate pAkt, neither of the treatments altered the expression of PHD2 in platelets significantly (Fig. 1e). We examined the effect of αKG on PI3K, activator of Akt. Our data show no significant effect of αKG on the expression of phosphorylated PI3K(p55) (Fig. S1c), thus, confirming that its specific target is pAkt.

4.3. Octyl αKG suppresses agonist-induced platelet activity, while PHD2 inhibitors augment it

Octyl αKG supplementation suppressed the expression of cell surface activation markers P-selectin, PS, PAC-1 binding to GP2b3a integrin on collagen-activated platelets (*P<0.05; Fig. 1j-l) and microparticle release from activated platelets (Fig. S3) in a concentration-dependent manner in vitro. In contrast, DKG enhanced the above parameters (*P<0.05, **P<0.01,***P<0.001; Fig. 1j-l). Similarly, αKG suppressed platelet aggregation induced by collagen (**P<0.01, ***P<0.001; Fig. 1m-n) or ADP (Fig. S4a-b) in a concentration-dependent manner, but DKG enhanced it (*P<0.05; Fig. 1m-n). Another PHD2 inhibitor DHB also enhanced collagen-induced platelet aggregation (*P<0.05, **P<0.01; Fig. S4j-k). Further, our data show that platelet thrombus formation was increased in a dose-dependent manner when whole blood was treated with DKG and perfused under flow shear condition on immobilized collagen surface. αKG significantly suppressed DKG-induced thrombus formation (****P<0.0001; Fig. 1o-p). Collagen-activated platelets secreted large amount of sphingosine-1-phosphate (S1P), a known stimulator of monocytes, which too was reduced by αKG supplementation (*P<0.05; Fig. 1q). Furthermore, our data show that DKG can rescue the suppressive effect of αKG on pAkt1(Thr308) (*P<0.05), and P-selectin and PS expression, and PAC-1 binding on platelets (*P<0.05) and platelet aggregation (**P<0.01, Fig. S4c-i).

4.4. Octyl αKG supplementation significantly suppresses monocyte functions by augmenting PHD2 activity

We then investigated the PHD2-mediated inhibition of pAkt1 (Thr308) in monocytes, isolated from healthy individuals and activated with either S1P or LPS after pre-treatment with octyl αKG *in vitro*. We show that the αKG supplementation decreased both Akt (Ser473) and pAkt1(Thr308) (*P<0.05, ****P<0.0001; Fig. 2a-c), and HIF1α and HIF2α (**P<0.01; Fig. 2a-c). Simultaneous suppression in secretion of inflammatory cytokines including, IL1β, IL6, TNFα and IL10 was observed (*P<0.05, **P<0.01,***P<0.001, ****P<0.0001; Fig. 2d-g). Similar outcomes were observed in monocytes exposed to LPS after pre-treatment of αKG (Fig. S5). We then confirmed that the above mechanism of αKG-induced suppression of monocyte activation is mediated primarily by pAkt, independent of HIFα. In HIF1α-depleted U937 monocytic cells (detailed protocol of shRNA-mediated depletion is described in Fig. S6), αKG supplementation significantly reduced cytokine secretion (*P<0.05; Fig. 2h-i) alongside down-modulated pAkt1(Thr308) (***P<0.001; Fig. 2j-k).

4.5. αKG-mediated suppression of pAkt in monocyte is mediated by PHD2

To confirm that αKG-mediated suppression of pAkt in monocyte is mediated by PHD2, we performed the above experiment in PHD2-

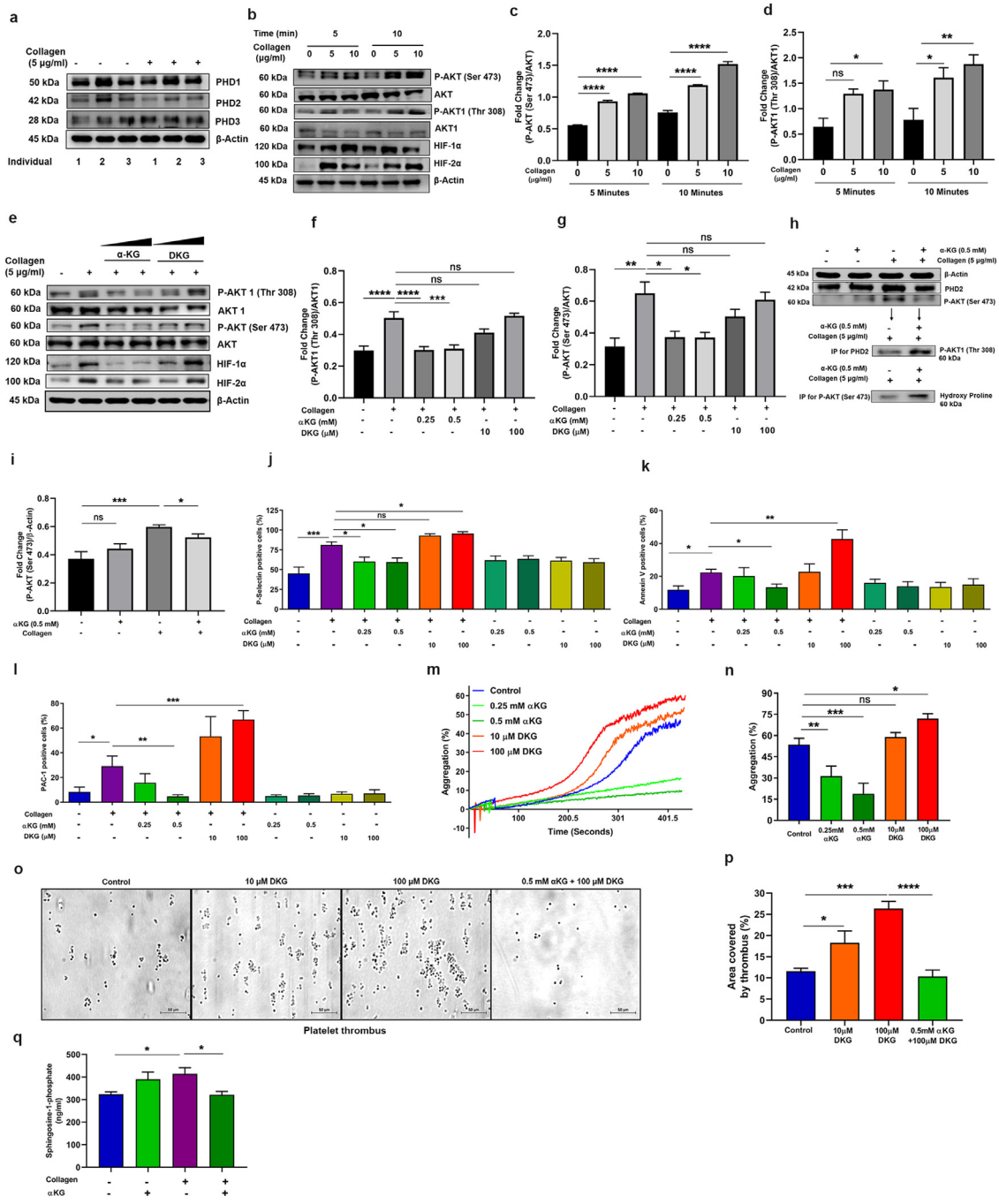

Fig. 1. αKG mediated augmentation of prolyl-hydroxylase activity of PHD2 inactivate pAkt in platelets. (**a**) All 3 isoforms of PHD exist in human platelet. Platelet-rich plasma (PRP) isolated from 3 different healthy individuals, after adjusting to equal number of platelets, was incubated with or without collagen (5 μg/ml) for 5 min and processed for western blotting (WB) of PHD1, PHD2 and PHD3. Densitometry data are mentioned in Fig. S14a. (**b-g**) PRP was incubated with collagen in a time- and concentration-dependent manner, and (b) expression of pAkt(Ser473), Akt, pAkt1(Thr 308), Akt1, HIF-1α and HIF-2α was measured in platelet pellet using WB. (c-d) Densitometry analysis shows elevated expression of pAkt and pAkt1 after collagen stimulation, other densitometry data are described in Fig. S14b-c. (e) Platelets were incubated with collagen in presence of αKG (0.25 and 0.5 mM) or DKG (10 and 100 μM) and the expression of above signalling molecules and PHD2 was measured using WB. (f-g) Densitometry data show suppression of collagen-induced elevation of pAkt and pAkt1 by αKG, but an elevation of these molecules in presence of DKG. Other densitometry data are described in Fig. S14d-f. (**h-i**) (h) Immunoprecipitation (IP) of PHD2 from lysate of washed-platelets from above experiment was performed and processed for WB of pAkt; further, IP of pAkt from same lysate and WB for hydroxy proline shows the interaction between the molecules. (i) Densitometry data of pAkt. Other densitometry data are described in Fig. S14g-h. (**j-k**) PRP from above experiment of Fig. 1c was processed for measuring surface (j) P-Selectin, (k) PS (Annexin-V binding) and (l) GP2b3a activation (PAC-1 binding) using flow cytometry. (**m-n**) (m) Platelet aggregation was performed using PRP pre-treated with αKG or DKG in response to collagen. (n) Percentage platelet aggregation was measured. Data from similar experiment in response to agonist ADP are described in Fig. S4. (**o-p**) (o) PRP from healthy individuals was incubated with αKG or DKG and perfused on immobilized collagen surface under arterial flow share condition 25 dyne/cm^2 and platelet thrombus formation was measured. Scale bar 50 μm. (p) Thrombus area was measured. (**q**) Secretion of Sphingosine-1-phosphate (S1P) was quantified from supernatant of αKG- and collagen-treated washed platelets using ELISA. Data in above figure are mean ± SEM from 3 independent experiments (one-way ANOVA, $^{*}P<0.05$. $^{**}P<0.01$, $^{***}P<0.001$, $^{****}P<0.0001$ and ns=non-significant).

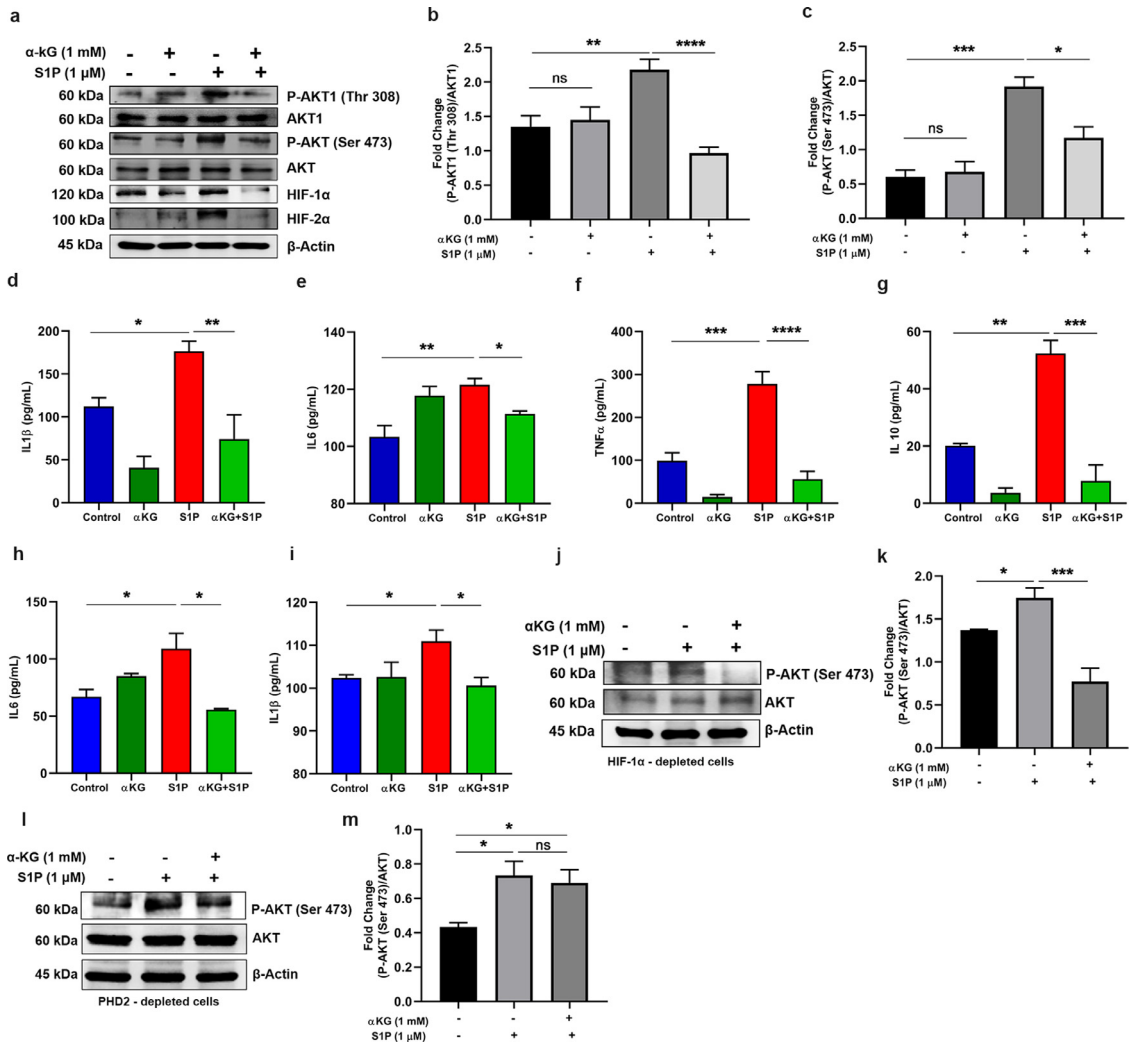

Fig. 2. αKG mediated elevation in prolyl-hydroxylase activity of PHD2 inhibits Akt phosphorylation in monocytes. (**a-c**) Monocytes isolated from healthy individuals were activated with Sphingosine 1 phosphate (S1P) with/without pre-treatment with αKG. (a) The expression of pAkt(Ser473), Akt, pAkt1(Thr 308), Akt1 HIF1α and HIF2α was measured using WB. (b-c) Densitometry data show suppression of S1P-induced elevation of pAkt and pAkt1 by αKG. Other densitometry data are described in Fig. S14i-j. Data from similar experiment using LPS as an agonist to monocytes, are described in Fig. S5. (**d-g**) The cytokines such as (d) IL1β, (e) IL6, (f) TNFα and (g) IL10, secreted by monocytes from above experiment, were measured using flow cytometry-based CBA array. (**h-k**) U937 monocytic cell line was depleted for *HIFA* (HIF1α) using shRNA (detailed protocol is described in Fig. S6) and treated with αKG before exposing to S1P treatment. (h) IL6 and (i) IL1β were measured from supernatant. (j-k) The cells from above experiment were used for measuring expression of pAkt and Akt using WB. (**l-m**) PHD2-depleted U937 monocytic cells were treated with αKG before exposing to S1P treatment and used for measuring expression of pAkt and Akt using WB. Data in above figure are mean ± SEM from 3 independent experiments (one-way ANOVA, $^{*}P<0.05$, $^{**}P<0.01$, $^{***}P<0.001$, $^{****}P<0.0001$ and ns= non-significant).

depleted U937 monocytic cells. Our data show that S1P-induced elevation of pAkt1 was not significantly suppressed by octyl αKG in PHD2-depleted cells (Fig. 2l-m), highlighting the role of PHD2 in the inactivation of pAkt1.

4.6. Elevated intracellular ratio of αKG to succinate augments activity of PHD2 in cells

To ascertain the mechanism of augmentation of PHD2 activity, we measured an elevated level of intracellular αKG in collagen-activated platelets after octyl αKG supplementation, even though the level was unaltered in collagen-activated platelets compared to resting platelets, in vitro ($^{*}P<0.05$; Fig. 3a). Since succinate, a product of αKG-dependent dioxygenase reaction in TCA cycle, inhibits PHD2 function, we measured its intracellular levels and found no significant change in platelets after collagen activation as well as post αKG supplementation (Fig. 3b). However, the intracellular αKG to succinate ratio was elevated in collagen-activated platelets after αKG supplementation, which might have played a role in augmentation of PHD2 activity ($^{*}P<0.05$, $^{**}P<0.01$; Fig. 3c) as suggested by others [37] as well as our recent work [34]. The intracellular level of other metabolites such as fumarate and pyruvate were found unaltered (Fig. S7a-b). We observed elevated lactate in supernatant of activated platelets, which levels of which were reduced by αKG supplementation ($^{*}P<0.05$; Fig. 3d).

We observed a similar elevation of intracellular αKG to succinate ratio in S1P-stimulated monocytes after octyl αKG supplementation, although the ratio was unaltered in S1P-activated monocytes compared to untreated monocytes ($^{*}P<0.05$, $^{**}P<0.01$, $^{***}P<0.001$; Fig. 3e-g), which might have played a role in augmentation of PHD2 activity.

4.7. Supplementation of dietary αKG significantly inhibits platelet aggregation in mice

We investigated whether the supplementation of dietary αKG inhibits platelet aggregation in mice, and observed that 1% αKG via drinking water for 24 and 48 hrs (experimental details are described in Fig. 4a) significantly inhibited platelet aggregation ex vivo, in

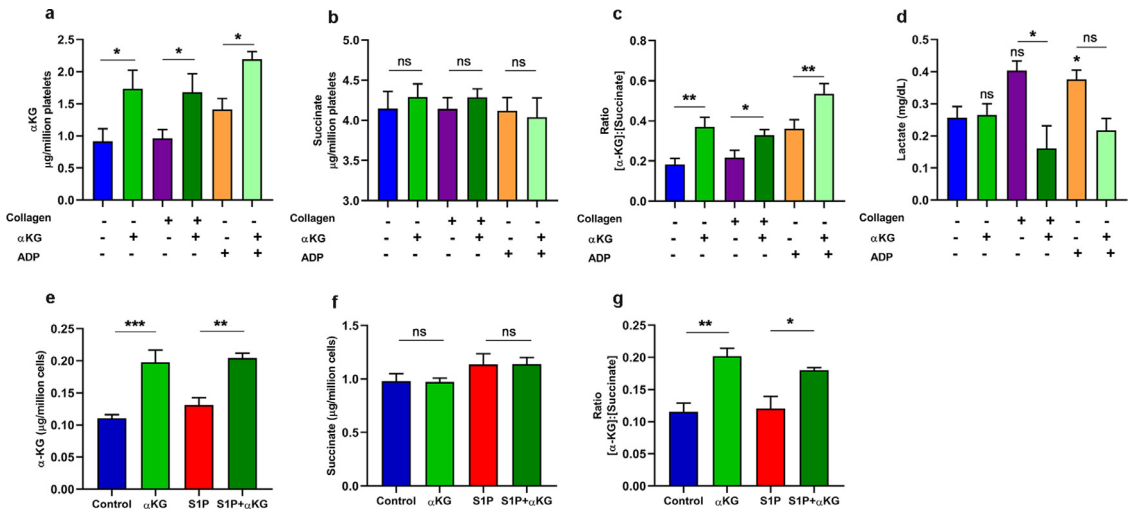

Fig. 3. Elevation in intracellular ratio of αKG to succinate promotes PHD2 activity in both platelet and monocyte. (**a-d**) PRP isolated from healthy individuals was pre-treated with αKG and activated in presence of collagen/ADP. Platelet pellet was washed and lysed, and used for measuring intracellular (a) αKG and (b) succinate using colorimetry-based assay. (c) Represents intracellular ratio of αKG to succinate. (d) Release of Lactate from supernatant of platelets from above experiment was quantified. Data of Pyruvate and Fumarate from platelet lysate is described in Fig. S7. (**e-f**) Similarly, intracellular (e) αKG and (f) succinate were measured from cell lysate of primary monocytes pre-treated with αKG and stimulated with S1P as described in Fig 2a. (g) Represents ratio of αKG to succinate in monocytes. Data in above figure are mean ± SEM from 3 independent experiments in duplicates (one-way ANOVA, $^{*}P<0.05$ and $^{**}P<0.01$, $^{***}P<0.001$ and ns=non-significant).

response to agonists such as collagen ($^{***}P<0.001$; Fig. 4b-c) and ADP ($^{*}P<0.05$, $^{**}P<0.01$; Fig. S9c). The above αKG supplementation did not alter the number of platelets and WBCs counts of mice (Fig. S8a-c), suggesting a feasible administration of this metabolite. In a recent work, we have described the safe rescue effect of 1% dietary αKG in mice exposed to hypoxia treatment [34].

4.8. Elevated intracellular ratio of αKG to succinate relates to PHD2 activity in platelets and monocytes in mice

We investigated the enzymatic activity of PHD2 in mice from above experiment. Our data show that the dietary αKG supplementation elevated αKG level in plasma ($^{**}P<0.01$; Fig. 4d) and also in platelets ($^{**}P<0.01$; Fig. 4e). An increased intracellular ratio of αKG to succinate in platelets ($^{*}P<0.05$; Fig. 4f-g) might have augmented PHD2 activity. Indeed, the decreased expression of pAkt1 ($^{**}P<0.01$) and HIF2α in platelets of αKG-supplemented mice has confirmed the augmented-activity of PHD2 (Fig. 4h-i). The platelets from αKG-supplemented mice had a reduced secretion of inflammatory mediator S1P ($^{**}P<0.01$; Fig. 4j). Similarly, PBMCs collected from αKG-supplemented mice had elevated level of intracellular αKG as well as αKG to succinate ratio ($^{*}P<0.05$; Fig. 4k-m). The PBMC of αKG-treated mice when exposed to stimulator like S1P in vitro, showed suppressed expression of pAkt and HIF2α ($^{**}P<0.01$; Fig. 4n-o). Based on these observations we further tested the effect of dietary αKG supplementation in animal models of induced thrombosis and inflammation.

4.9. Dietary αKG significantly inhibits carrageenan-induced thrombosis and inflammation in mice

Dietary supplementation of αKG (starting at 24 or 48 hrs before carrageenan treatment) significantly reduced tail thrombosis ($^{**}P<0.01$; Fig. 5b-c) and clot formation in lungs and liver ($^{**}P<0.01$, $^{***}P<0.001$, $^{****}P<0.0001$; Fig. 5d-g, and S10a-b), and platelet accumulation in lungs ($^{***}P<0.001$; Fig. S10c-d). We also found decrease in accumulation of leukocytes in lungs of carrageenan-treated mice supplemented with αKG ($^{**}P<0.01$, $^{****}P<0.0001$; Fig. 5h-i, Fig. S11). αKG supplementation also suppressed the levels of inflammatory cytokines such as IL1ß, IL6 and TNFα in plasma of carrageenan treated mice ($^{*}P<0.05$,$^{**}P<0.01$, $^{***}P<0.001$, $^{****}P<0.0001$; Fig. 5j-m). Besides, αKG-supplemented mice when treated with carrageenan locally at abdomen and for a short period (3 and 6 hrs), displayed a decreased release of myeloperoxidase (MPO) ($^{*}P<0.05$, $^{****}P<0.0001$; Fig. 5n-p) and less accumulation of monocytes, neutrophils and leukocyte-platelet aggregates ($^{*}P<0.05$,$^{**}P<0.01$, $^{***}P<0.001$, $^{****}P<0.0001$; Fig. 5q-t; Fig. S12b-c) in the peritoneum.

4.10. Dietary αKG significantly inhibits inflammation and thrombosis alongside downmodulation of pAkt in lung of the hamsters infected with SARS-CoV-2

A recent report described the increased expression of pAkt1 (Thr308) in human alveolar epithelial type 2 cells after SARS-CoV-2 infection [17]. We also observed a similar elevated expression of pAkt1(Thr308) in human liver Huh7 cell line infected with this virus. As expected, we observed a significant reduction in pAkt1(Thr308) expression ($^{***}P<0.001$, $^{****}P<0.0001$; Fig. 6a-b) along with decreased IL6 secretion ($^{*}P<0.05$; Fig. 6c) in these infected cells after octyl-αKG supplementation, but viral load did not change significantly (Fig. 6d). No change in expression of PHD2 was observed in Huh7 cells after viral infection as well as after αKG treatment (Fig. 6a). We then tested the rescue effect of dietary αKG (1%), administered via drinking water and oral gavage (protocol of treatment is described in Fig. 6e). We observed significantly reduced evidence of lung thrombi in SARS-CoV-2 infected hamsters (Fig. 6f). The histopathology data showed a significantly reduced intravascular clot formation ($^{*}P<0.05$; Fig. 6g-h) and leukocyte accumulation in alveolar spaces ($^{****}P<0.0001$; Fig. 6i-j) in the lung of SARS-CoV-2 infected hamsters after αKG administration. The elevated expression of pAkt in lung of SARS-CoV-2 infected animals was significantly reduced after αKG supplementation ($^{**}P<0.01$; Fig. 6k-l). The elevated expression of HIF2α in lungs of SARS-CoV-2 infected animals was also significantly reduced after αKG supplementation ($^{**}P<0.01$; Fig. S13a-b). The body weight decreased significantly in infected animals during day 3 - 6, but no rescue effect of αKG on body weight was observed (Fig. 6m). As reported by others, [30] we did not observe death of SARS-CoV-2 infected hamsters. We also observed a gradual increase in body weight, day 8 onwards in another group of all infected hamsters. However, a decreased viral load in lungs was observed on day 6 in infected animals supplemented with αKG ($^{*}P<0.05$; Fig. 6n). Supplementation with 1% dietary αKG for 6 days to control hamsters did not alter the number of blood cells including

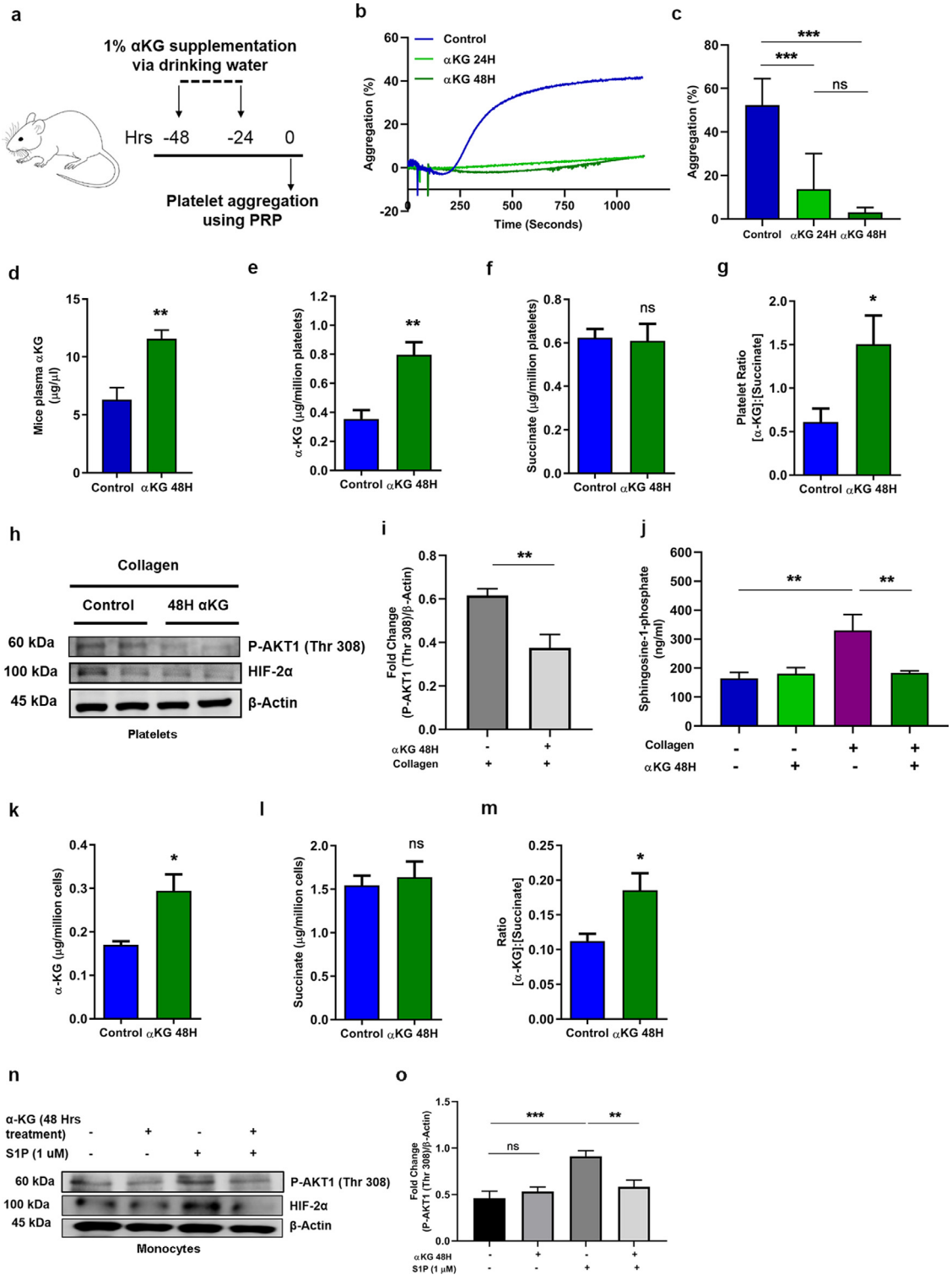

Fig. 4. Dietary *αKG* supplementation to healthy wild type mice reduces platelet and monocyte activation. (**a**) Schematic showing experimental protocol. BALB/c mice were supplemented with dietary *α*KG for 24 and 48 hrs, and whole blood was isolated to separate PRP for assessing following parameters. (**b-c**) (b) Percentage platelet aggregation in presence of collagen or ADP (ADP data in Fig. S9). (c) Percentage platelet aggregation from 8 mice in each group (one-way ANOVA, $^{***}P<0.001$ and ns=non-significant). (**d-g**) (d) Plasma concentration of *α*KG was quantified from above mice, control vs. 48 hrs *α*KG groups (n=8). The intracellular (e) *α*KG and (f) succinate and their (g) fold change ratio in platelets of mice pre-treated with/without *α*KG for 48 hours (n=8) (unpaired t-test, $^{*}P<0.05$, $^{**}P<0.01$ and ns=non-significant). (**h-i**) (h) Expression of pAkt1(Thr 308), HIF-2*α* was measured in platelets from mice of above groups using WB. Representative image shows blot from 2 mice. (i) Densitometry data show suppression of collagen-induced elevation of pAkt1(Thr 308) in *α*KG treated mice (n=8) (unpaired t-test, $^{**}P<0.01$). Other densitometry data in Fig. S14k. (**j**) S1P secretion was measure from supernatant of collagen-activated platelets of above mice groups (n=8) (one-way ANOVA, $^{**}P<0.01$). (**k-m**) Similarly, the intracellular (k) *α*KG and (l) succinate and their (m) fold change ratio in PBMCs was detected from above mice (n=8) (unpaired t-test, $^{*}P<0.05$ and ns=non-significant). (**n-o**) (n) Expression of pAkt1(Thr 308), HIF-2*α* was measured in PBMCs from above mice, after treating the cells with S1P *ex vivo*. Representative image shows blot from a mouse. (o) Densitometry data show suppression of S1P-induced elevation of pAkt in *α*KG treated mice (n=8) (one-way ANOVA, $^{*}P<0.05$, $^{**}P<0.01$, $^{****}P<0.0001$). Other densitometry data in Fig. S14l. Data in above figure are mean ± SEM from 3 independent experiments.

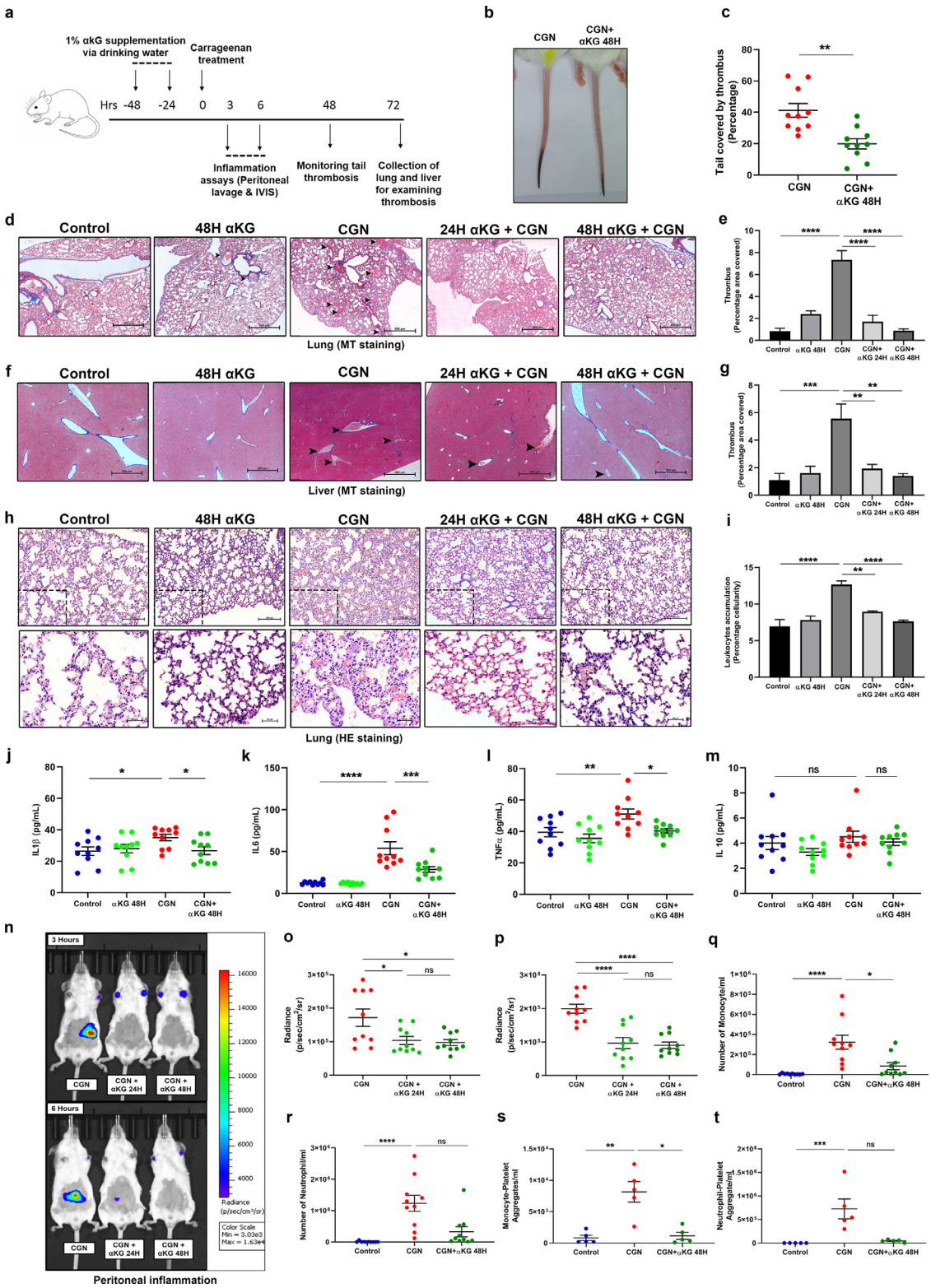

Fig. 5. Dietary αKG supplementation rescues mice from carrageenan-induced thrombosis and inflammation. (**a**) Schematic showing experimental protocol. BALB/c mice were supplemented with dietary αKG before exposed to carrageenan treatment and following parameters were assessed. (**b-c**) (b) Tail thrombosis was measured, showing a representative image. (c) Percentage thrombosis. Each dot represents a mouse (unpaired t-test, $^{**}P<0.01$). (**d-g**) (d-e) Lung and (f-g) Liver section from above mice groups were used for assessing clot formation using Masson-trichrome (MT) staining. Scale bar 500 μm. Percentage covered area of clot was measured. The haematoxylin and eosin (H&E) staining data of similar observations are described in Fig. S10. (**h-i**) Similarly, H&E staining of lung was used for assessing leukocyte accumulation. Score is calculated as percentage cellularity. Scale bar 500 μm and 20 μm. Showing reduced inflammation in αKG-treated mice (one-way ANOVA, $^{**}P<0.01$, $^{***}P<0.001$ and $^{****}P<0.0001$). The MT staining data of similar observations are described in Fig. S11. Fig. d-i, n=8. (**j-m**) Cytokines (j) IL1β, (k) IL6, (l) TNFα and (m) IL10 were measured from mice groups (one-way ANOVA, $^{*}P<0.05$, $^{**}P<0.01$, $^{***}P<0.001$, $^{****}P<0.0001$ and ns=non-significant). (**n-t**) To measure local inflammation αKG-supplemented mice were injected with carrageenan at peritoneum region and (n) luminescence generated from MPO-luminol interaction were measured using IVIS imaging system to assess leukocyte activation and inflammation. Radiance count from (o) 3 and (p) 6 hours post carrageenan treatment. αKG-supplemented mice displayed reduced MPO signal intensity (one-way ANOVA, $^{*}P<0.05$, $^{****}P<0.0001$ and ns=non-significant). (q) Monocytes, (r) neutrophils, (s) monocytes-platelet and (t) neutrophil-platelet aggregates were measured from peritoneum lavage of above treated mice. Each dot represents a mouse (Kruskal Wallis test, $^{*}P<0.05$, $^{**}P<0.01$, $^{***}P<0.001$, $^{****}P<0.0001$ and ns=non-significant). Data in above figure are mean ± SEM from different experiments.

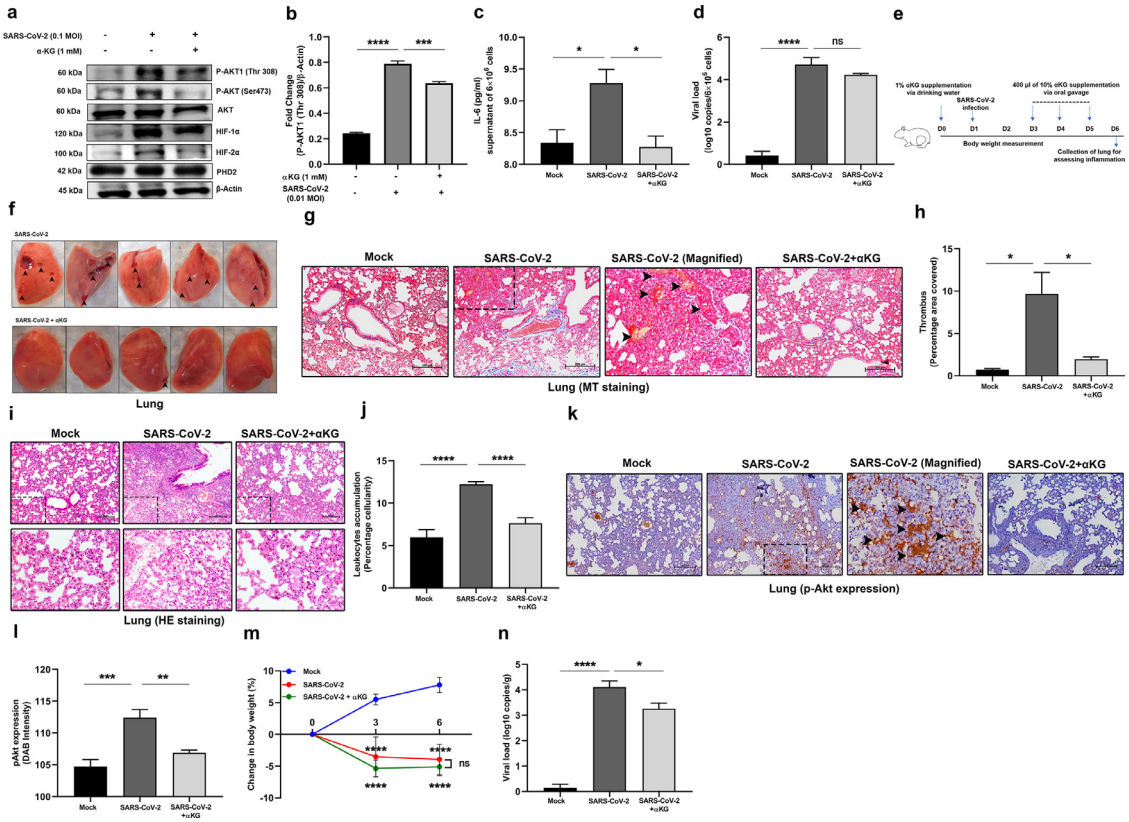

Fig. 6. Dietary αKG supplementation rescues hamsters from SARS-CoV-2 induced lung thrombosis and inflammation. (**a-b**) Before performing *in vivo* study we performed *in vitro* experiment and infected human liver Huh7 cell line with 0.1 MOI of SARS-CoV-2 for 24 hrs with a prior treatment with 1mM octyl-αKG. (a) We assessed pAkt1(Thr308) expression using WB. (b) Densitometry analysis from three independent experiments shows elevated expression of pAkt1(Thr308), other densitometry data are described in Fig. S14m-p. (**c**) IL6 level was measured from supernatant of SARS-CoV-2 infected Huh7 cells from above experiment. (**d**) SARS-CoV-2 genome was measured from above cell pellet using RT-PCR. (**e**) Schematic Figure shows the experimental protocol using hamsters. (**f**) Lung was isolated and imaged, showing clot injury spot (arrows) after viral infection, which was rescued to almost normal condition with αKG supplementation. (**g-h**) (g) Lung section from above mice groups were used for assessing clot formation and collagen deposition using MT staining and (h) Percentage covered area of thrombus was measured. (**i-j**) (i) H&E staining of lung was used for assessing leukocyte accumulation in lung including alveolar spaces as the marker of inflammation. (Lower panel) magnified version from upper panel images. (j) Score is calculated as percentage cellularity. Showing reduced inflammation in αKG-treated animals. (**k-l**) (k) The sections were labelled with pAkt antibody and stained with HRP-conjugated secondary antibody. (l) pAkt expression was quantified by measuring DAB staining (brown), which was increased in virus infection and decreased after αKG treatment. (g-l) Image scale bar 200 µm and number of animals used n=5 in mock, n=9 each in other groups. (**m**) Body weight of the animals were measured at day 0, 3 and 6, and calculated as mean ± SD, n=5 in mock, n=11 each in other groups (two-way ANOVA, $^{****}P<0.0001$ and ns=non-significant). (**n**) SARS-CoV-2 genome was measured from lung tissue (gram) of hamsters using RT-PCR, n=3 in mock, n=11 each in other groups. In all figures other than Fig. 6m, data are mean ± SEM from independent experiments (one-way ANOVA, $^{*}P<0.05$, $^{**}P<0.01$, $^{***}P<0.001$, $^{****}P<0.0001$ and ns=non-significant).

platelet, WBCs and granulocytes (Fig. S8d-f), suggesting a safe implementation of the metabolite.

5. Discussion

Our study for the first time describes the regulatory role of PHD2-pAkt axis in platelet function. We report an inactivating impact of α-ketoglutarate (αKG) mediated augmentation of prolyl hydroxylation activity of PHD2 on phosphorylated Akt1 (pAkt1). An earlier study has described that pAkt1 undergoes prolyl hydroxylation at Pro125 and Pro313, by PHD2, in a reaction decarboxylating αKG. Hydroxylated pAkt1(Thr308) is dephosphorylated by Von Hippel-Lindau protein (pVHL) associated protein phosphatase 2A (PP2A), leading to Akt inactivation. Study thus unveiled this pathway as another mechanism of post translational modification for pAkt, and described that in VHL-deficient/suppressed setting and under hypoxic microenvironment, accumulation of pAkt is likely to promote tumour growth and its inhibition partially reverses the effect [25].

We describe here that the supplementation with αKG, an intermediate of TCA cycle, significantly suppresses pAkt1 and reduces agonist-induced platelet activation under normoxia. Upon activation by agonists like collagen [3] and ADP [38] platelets undergo Akt phosphorylation by PDK1. Akt phosphorylation is known to stimulate cell surface adhesion molecules like GP2b3a and GPVI, and promote platelet aggregation, adhesion, and secretion of granular contents [39,40]. αKG supplementation significantly inhibits these functions of platelets by suppressing pAkt1. In contrast, a marked amplification in platelet activity alongside increased pAkt1 was observed after treatment with PHD2 inhibitors like DKG or DHB. This indicates a crucial involvement of PHD2 in the regulation of platelet activation. This conclusion was further supported by the αKG-mediated attenuation of HIF1α and HIF2α expression, known substrates of PHD2, and there by DKG/DHB-driven stabilization. Augmented PHD2 activity orchestrated these events as confirmed by increased hydroxylated proline alongside enhanced binding of PHD2 to pAkt in αKG-treated platelets. Further, our study also describes an increased intracellular αKG: succinate ratio in platelets after αKG supplementation. PHD2 catalyses proline hydroxylation of its substrates by converting O_2 and αKG to CO_2 and succinate, [41] and succinate can inhibit PHD2 by competing with αKG [42] Therefore, an elevated intracellular ratio of αKG to succinate may serve as a stimulator of PHD2 activity [37] It is notable that αKG: succinate ratio was unaltered in platelets after activation with agonist, but its elevated ratio in αKG-supplemented platelets significantly augmented PHD2 activity and in turn downmodulated pAkt1. However, several studies have reported increased pAkt in platelets and other cells in vitro [43,44] and in vivo [45] after succinate supplementation. This suggests that intracellular ratio of these two metabolites serves as a switch for the PHD2 activity. We show that

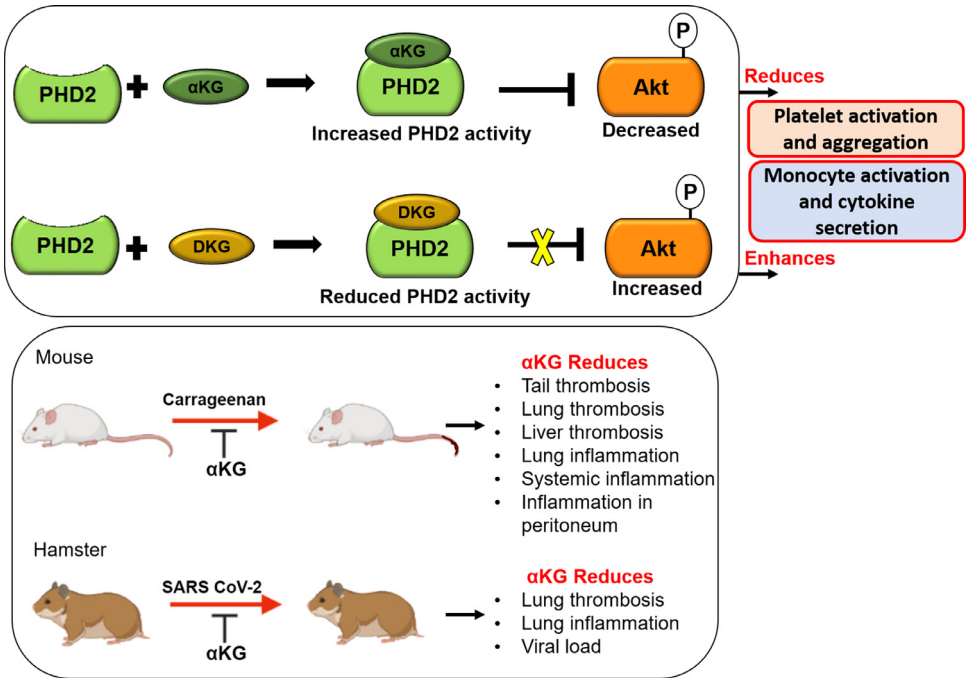

Fig. 7. αKG mediated suppression of platelet and monocyte functions. Schematic depicts that under normoxic environment supplementation with αKG (known cofactor of PHD2) increases PHD2 activity by elevating intracellular αKG: succinate ratio. Elevated PHD2 activity degrades pAkt1 and reduces platelet activation and aggregation. A similar mechanism also suppresses inflammatory function of monocytes. Thus, suggesting the involvement of αKG-PHD2-Akt1 axis in the regulation of events like thrombosis and inflammation. Importantly, dietary αKG supplementation significantly rescues mice from carrageenan-induced clot formation, and leukocyte accumulation and inflammation in various organs including lung. Importantly, dietary αKG rescues significantly hamsters from SARS-CoV-2 induced clot formation and leukocyte accumulation in the lung, alongside downmodulation of pAkt.

αKG supplementation significantly decreased platelet's pAkt and inhibited aggregation, thrombus formation and secretion of granular contents including inflammatory mediator sphingosin-1 phosphate (S1P), in vitro. S1P is an intermediary between platelet activation and inflammation as it activates monocytes. We observed that αKG could also suppress S1P-mediated activation of monocytes in a pAkt1 dependent manner. When LPS was used as an activator to simulate a thrombo-inflammatory condition, αKG could deter the secretion of pro-inflammatory cytokines from monocytes. Importantly, our data showed no significant inactivation of pAkt1 by αKG in PHD2-deficient monocytic cell line, thus confirming that αKG imparts its effects primarily through PHD2. Overall, our data upholds PHD2 as a potential target to abrogate Akt signalling. Other studies have extensively used antagonists/inhibitors to target pathological signalling of Akt or PI3K-Akt to inhibit thrombosis and inflammation [8,4,23-24].

Our study underscores the implementation of dietary αKG supplementation to mice as a promising treatment to reduce the platelet aggregation and inflammatory response of monocytes by downmodulating pAkt1 without altering the number of these cell types, thus suggesting a safe administration of this metabolite. In a separate study, we have described a rescue effect of this metabolite in mice from hypoxia-induced inflammation by downmodulating HIF1/2α and NFκB [34]. Another recent study has mentioned the induction of IL10 by dietary αKG and suppression of chronic inflammation in mice [46]. αKG suppresses the NFκB mediated inflammation in piglets [47]. αKG has been used extensively for in vivo experimental therapies for manipulating multiple cellular processes related to organ development and viability of organisms, [48,49] restriction of tumour growth and extending survival, [50] and preventing obesity [51].

We also describe the αKG-mediated rescue of clot formation and leukocyte accumulation alongside a reduction in cytokine secretion by these cells in lungs and other organs in mice exposed to a thrombosis-inducing agent like carrageenan. Furthermore, our study also reports a significant rescue effect of αKG on inflamed lung in SARS-CoV-2 infected hamsters along with significant reduction in intravascular clot formation, prevention of accumulation of leukocytes including macrophages and neutrophils in alveolar spaces of the lung of infected hamsters. This indicates that αKG usage can decelerate inflammation induced lung tissue damage in severe cases of SARS-CoV-2 infection and may eventually delay or even abrogate the development of acute respiratory distress syndrome (ARDS), a known symptom of COVID-19 [52,53]. However, more experimental evidence will be needed before the implementation of this metabolite in this clinical scenario. The αKG administration also decreased viral load in lungs of the infected animals along with concomitant decrease in pAkt. The exact role Akt in replication of SARS-CoV-2 remains to be delineated; but it has been reported in other viruses [54] However, a recent study has described an elevated pAkt1 (Thr308) in cells infected with SARS-CoV-2 [17]. Our in vitro data also show an elevated pAkt1(Thr308) alongside increased IL6 secretion by SARS-CoV-2 infected Huh7 cell line, which was further inhibited by αKG administration. All these observations underscore that the augmentation of PHD2 activity by αKG could be a potential therapeutic strategy to inhibit pAkt-mediated maladies like inflammation and thrombosis, as well as possible propagation of SARS-CoV-2.

We depict a novel role of PHD2-pAkt axis in the regulation of platelet and leukocyte functions. Supplementation with αKG significantly increases the hydroxylase activity of PHD2 and therefore reduces phosphorylation of Akt and in turn suppresses thrombotic and inflammatory functions of platelets and leukocytes respectively (schematic Figure 7). We propose a safe implementation of dietary αKG in prevention of Akt-driven thrombosis and inflammation in various disease scenarios including inflamed lung of COVID-19 patients.

6. Some of the limitations of our study

- In Fig 5, we used carrageenan-induced thrombosis mice model. We did not have access to more widely used thrombosis mice models such as $FeCL_3$-induced mesenteric arteriole thrombosis model.

- We did not have access to use mice models of SARS-CoV-2 infection. We used hamster, which is also an established model for SARS-CoV-2 infection. The detailed inflammatory markers including specific immunes cells and cytokines were not assessed due to limitation in availability of these reagents.

7. Contributors

NMS designed and performed all experiments, analysed data and wrote the manuscript. SA designed and performed mice experiment for immunophenotyping and histochemistry and analysed related data. SK and Sankar B designed and performed COVID-19 infection studies, and Sankar B has supervised the infection experiments. Sulagna B designed and performed metabolite estimation experiments, analysed and interpreted data, and edited the manuscript. JTP provided crucial conceptual inputs and edited the manuscript. PG designed and supervised the study, conceptualized the approach, designed the experiments, analyzed the data, and wrote the manuscript. All authors read, edited and approved the final manuscript.

8. Data sharing

The materials described in the manuscript, including all relevant raw data will be freely available from the corresponding author.

Supplementary Materials

Fig. S1: Measuring: Akt1 phosphorylation (pAkt1) in platelet induced by ADP; agonist induced pAkt1 in platelet in presence of PHD2 inhibitor DHB; and pPI3K inn presence of αKG.

Fig. S2: IgG control for immunoprecipitation of PHD2 and P-Akt from platelet lysate.

Fig. S3: Microparticle release from platelets after αKG treatment.

Fig. S4: ADP induced platelet aggregation in presence of αKG, DKG and DHB. DKG rescues αKG-mediated suppression of platelet activation and aggregation.

Fig. S5: Effect of αKG on LPS induced HIF-2α and P-Akt expression in monocytes.

Fig. S6: Generation of HIF-1α depleted cells.

Fig. S7: Measuring intracellular level of fumarate and pyruvate in activated platelets after αKG supplementation.

Fig. S8: Mice and hamster blood counts after dietary αKG supplementation.

Fig. S9: In vitro platelet aggregation in presence of octyl αKG, platelets were collected from normal mice; and platelet aggregation collected from αKG treated mice.

Fig. S10: H&E staining of mice lung and liver showing reduction of carrageenan induced thrombosis by dietary α-KG supplementation. Immunostaining of platelet marker in the lung sections from above experiment.

Fig. S11: Masson's trichrome (MT) staining of mice lung showing reduction of leukocyte infiltration in carrageenan-treated mice after dietary αKG supplementation.

Fig. S12: Gating strategy for immune cells from mice peritoneal lavage fluid.

Fig. S13: HIF-2α expression in lung tissue of hamsters infected with SARS-CoV-2.

Fig. S14: Densitometry of Western blots.

Supplementary Table S1: List of antibodies used in the study. Supplementary Table S2: List of reagents used in the study.

Declaration of Competing Interest

Authors declare that there is no conflict of interest.

Acknowledgements

Authors acknowledge generous help of Prof. Sudhanshu Vrati of Regional Centre for Biotechnology, Faridabad, India for sharing SARS-CoV-2 virus strain. Authors acknowledge Dr. Arundhati Tiwari, Department of Biochemistry, Institute of Medical Sciences, Banaras Hindu University, India for editing the manuscript. Authors also acknowledge the funding by grants: BT/PR22881 and BT/PR22985 from the Department of Biotechnology (DBT), Govt. of India; and CRG/000092 from the Science and Engineering Research Board, Govt. of India to PG.

Supplementary materials

Supplementary material associated with this article can be found in the online version at doi:10.1016/j.ebiom.2021.103672.

References

[1] Dittrich M, Birschmann I, Mietner S, Sickmann A, Walter U, Dandekar T. Platelet protein interactions: Map, signalling components, and phosphorylation ground state. Arterioscler Thromb Vasc Biol 2008;28(7):1326–31.
[2] Woulfe D, Jiang H, Morgans A, Monks R, Birnbaum M, Brass LF. Defects in secretion, aggregation, and thrombus formation in platelets from mice lacking Akt2. J Clin Invest 2004;113(3):441–50.
[3] Chen J, De S, Damron DS, Chen WS, Hay N, Byzova TV. Impaired platelet responses to thrombin and collagen in AKT-1-deficient mice. Blood 2004;104(6):1703–10.
[4] Yin H, Stojanovic A, Hay N, Du X. The role of Akt in the signalling pathway of the glycoprotein Ib-IX-induced platelet activation. Blood 2008;111(2):658–65.
[5] O'Brien KA, Stojanovic-Terpo A, Hay N, Du X. An important role for Akt3 in platelet activation and thrombosis. Blood 2011;118(15):4215–23.
[6] Stojanovic A, Marjanovic JA, Brovkovych VM, Peng X, Hay N, Skidgel RA, et al. A phosphoinositide 3-kinase-AKT-nitric oxide-cGMP signalling pathway in stimulating platelet secretion and aggregation. J Biol Chem 2006;281(24):16333–9.
[7] O'Brien KA, Gartner TK, Hay N, Du X. ADP-stimulated activation of akt during integrin outside-in signalling promotes platelet spreading by inhibiting glycogen synthase kinase-3β. Arterioscler Thromb Vasc Biol 2012;32(9):2232–40.
[8] Reséndiz JC, Kroll MH, Lassila R. Protease-activated receptor-induced Akt activation - Regulation and possible function. J Thromb Haemost 2007;5(12):2484–93.
[9] Holinstat M, Preininger AM, Milne SB, Hudson WJ, Brown HA, Hamm HE. Irreversible platelet activation requires protease-activated receptor 1-mediated signalling to phosphatidylinositol phosphates. Mol Pharmacol 2009;76(2):301–13.
[10] Camps M, Rückle T, Ji H, Ardissone V, Rintelen F, Shaw J, et al. Blockade of PI3Kγ suppresses joint inflammation and damage in mouse models of rheumatoid arthritis. Nat Med 2005;11:936–43.
[11] Sospedra M, Martin R. Immunology of Multiple Sclerosis. Semin Neurol 2016;36(2):115–27.
[12] Busse WW, Lemansk RFJR. Epidemiologic and clinical observations have linked IgE antibodies to the severity of asthma 13 and the initial and sustained responses of the airway to allergens. 14 To initiate the synthesis of IgE, inhaled allergens must. English J 2001;344(5):350–62.
[13] Shapiro SD. COPD unwound. N Engl J Med 2005;352(19):2016–9.
[14] Schön MP, Boehncke WH. Medical Progress: Psorasis. N Engl J Med 2005;352:1899–912.
[15] Fernández-Hernando C, Ackah E, Yu J, Suárez Y, Murata T, Iwakiri Y, et al. Loss of Akt1 Leads to Severe Atherosclerosis and Occlusive Coronary Artery Disease. Cell Metab 2007;6(6):446–57.
[16] Paez J, Sellers WR. PI3K/PTEN/AKT pathway. A critical mediator of oncogenic signalling. Cancer Treat Res 2003;115:145–67.
[17] Hekman RM, Hume AJ, Goel RK, Abo KM, Huang J, Blum BC, et al. Actionable Cytopathogenic Host Responses of Human Alveolar Type 2 Cells to SARS-CoV-2. Mol Cell 2020;80(6):1104–22.
[18] Bouhaddou M, Memon D, Meyer B, White KM, Rezelj VV, Correa Marrero M, et al. The Global Phosphorylation Landscape of SARS-CoV-2 Infection. Cell 2020;182(3):685–712.
[19] Mizutani T, Fukushi S, Saijo M, Kurane I, Morikawa S. Importance of Akt signalling pathway for apoptosis in SARS-CoV-infected Vero E6 cells. Virology 2004;327(2):169–74.
[20] Lee CJ, Liao CL, Lin YL. Flavivirus activates phosphatidylinositol 3-kinase signalling to block caspase-dependent apoptotic cell death at the early stage of virus infection. J Virol 2005;79:8388–99.
[21] Hanada M, Feng J, Hemmings BA. Structure, regulation and function of PKB/AKT - A major therapeutic target. Biochim Biophys Acta - Proteins Proteomics 2004;1697(1-2):3–16.
[22] Di Lorenzo A, Fernández-Hernando C, Cirino G, Sessa WC. Akt1 is critical for acute inflammation and histamine-mediated vascular leakage. Proc Natl Acad Sci U S A 2009;106(34):14552–7.
[23] Pengal RA, Ganesan LP, Wei G, Fang H, Ostrowski MC, Tridandapani S. Lipopolysaccharide-induced production of interleukin-10 is promoted by the serine/threonine kinase Akt. Mol Immunol 2006;43(10):1557–64.

[24] Nandy D, Janardhanan R, Mukhopadhyay D, Basu A. Effect of hyperglycemia on human monocyte activation. J Investig Med 2011;59(4):661–7.
[25] Guo J, Chakraborty AA, Liu P, Gan W, Zheng X, Inuzuka H, et al. pVHL suppresses kinase activity of Akt in a proline- hydroxylation–dependent manner. Science 2017;353(6302):929–32.
[26] Hagimori M, Kamiya S, Yamaguchi Y, Arakawa M. Improving frequency of thrombosis by altering blood flow in the carrageenan-induced rat tail thrombosis model. Pharmacol Res 2009;60:320–3.
[27] Zhang S, Liu Y, Wang X, Yang L, Li H, Wang Y, et al. SARS-CoV-2 binds platelet ACE2 to enhance thrombosis in COVID-19. J Hematol Oncol 2020;13(1):120.
[28] Manne BK, Denorme F, Middleton EA, Portier I, Rowley JW, Stubben C, et al. Platelet gene expression and function in patients with COVID-19. Blood 2020;136 (11):1317–29.
[29] Pamukcu B. Inflammation and thrombosis in patients with COVID-19: A prothrombotic and inflammatory disease caused by SARS coronavirus-2. Anatol J Cardiol 2020;24:224–34.
[30] Sia SF, Yan LM, Chin AWH, Fung K, Choy KT, Wong AYL, et al. Pathogenesis and transmission of SARS-CoV-2 in golden hamsters. Nature 2020;583:834–8.
[31] Singhal R, Annarapu GK, Pandey A, Chawla S, Ojha A, Gupta A, et al. Hemoglobin interaction with GP1bα induces platelet activation and apoptosis: A novel mechanism associated with intravascular hemolysis. Haematologica 2015;100 (12):1526–33.
[32] Bhasym A, Annarapu GK, Saha S, Shrimali N, Gupta S, Seth T, et al. Neutrophils develop rapid proinflammatory response after engulfing Hb-activated platelets under intravascular hemolysis. Clin Exp Immunol 2019;197(2):131–40.
[33] Annarapu GK, Singhal R, Gupta A, Chawla S, Batra H, Seth T, et al. HbS Binding to GP1bα Activates platelets in sickle cell disease. PLoS One 2016;11(12):1–12.
[34] Bhattacharya S, Shrimali NM, Mohammad G, Koul PA, Prchal JT, Guchhait P. Gain-of-function Tibetan PHD2$^{D4E;C127S}$ variant suppresses monocyte function: A lesson in inflammatory response to inspired hypoxia. EBioMedicine 2021;68:103418.
[35] Torres-Rêgo M, Furtado AA, Bitencourt MAO, Lima MCJS, Andrade RCLC, Azevedo EP, et al. Anti-inflammatory activity of aqueous extract and bioactive compounds identified from the fruits of Hancornia speciosa Gomes (Apocynaceae). BMC Complement Altern Med 2016;16:1–10.
[36] Ghosn EE, Cassado AA, Govoni GR, Fukuhara T, Yang Y, Monack DM, et al. Two physically, functionally, and developmentally distinct peritoneal macrophage subsets. Proc Natl Acad Sci U S A 2010;107:2568–73.
[37] MacKenzie ED, Selak MA, Tennant DA, Payne LJ, Crosby S, Frederiksen CM, et al. Cell-Permeating α-Ketoglutarate Derivatives Alleviate Pseudohypoxia in Succinate Dehydrogenase-Deficient Cells. Mol Cell Biol 2007;27(9):3282–9.
[38] Kim S, Foster C, Lecchi A, Quinton TM, Prosser DM, Jin J, et al. Protease-activated receptors 1 and 4 do not stimulate Gi signalling pathways in the absence of secreted ADP and cause human platelet aggregation independently of Gi signalling. Blood 2002;99(10):3629–36.
[39] Shattil SJ, Newman PJ, Dc W. Integrins : dynamic scaffolds for adhesion and signalling in platelets Integrins : dynamic scaffolds for adhesion and signalling in platelets. Blood 2004;104(6):1606–15.
[40] Woulfe DS. Akt signalling in platelets and thrombosis. Expert Rev Hematol 2010;3 (1):81–91.
[41] Kaelin WG, Ratcliffe PJ. Oxygen Sensing by Metazoans: The Central Role of the HIF Hydroxylase Pathway. Mol Cell 2008;30(4):393–402.
[42] Gorres KL, Raines RT. Prolyl 4-Hydroxylase. Crit Rev Biochem Mol Biol 2010;45 (2):106–24.
[43] Högberg C, Gidlöf O, Tan C, Svensson S, Nilsson-Öhman J, Erlinge D, et al. Succinate independently stimulates full platelet activation via cAMP and phosphoinositide 3-kinase-b signalling. J Thromb Haemost 2011;9:361–72.
[44] Wang T, Xu YQ, Yuan YX, Xu PW, Zhang C, Li F, et al. Succinate induces skeletal muscle fiber remodeling via SUCNR1 signalling. EMBO Rep 2020;21:e50461.
[45] Yang L, Yu D, Mo R, Zhang J, Hua H, Hu L, et al. The Succinate Receptor GPR91 Is Involved in Pressure Overload-Induced Ventricular Hypertrophy. PLoS One 2016;11:e0147597.
[46] Asadi SA, Edgar D, Liao CY, Hsu YM, Lucanic M, Asadi SA, et al. Alpha-Ketoglutarate, an Endogenous Metabolite, Extends Lifespan and Compresses Morbidity in Aging Mice. Cell Metab 2020;32:447–56.
[47] He L, Li H, Huang N, Zhou X, Tian J, Li T, et al. Alpha-ketoglutarate suppresses the NF-κB-mediated inflammatory pathway and enhances the PXR-regulated detoxification pathway. Oncotarget 2017;8:102974–88.
[48] Chin RM, Fu X, Pai MY, Vergnes L, Hwang H, Deng G, et al. The metabolite α-ketoglutarate extends lifespan by inhibiting ATP synthase and TOR. Nature 2014;510 (7505):397–401.
[49] Wang Y, Deng P, Liu Y, Wu Y, Chen Y, Guo Y, et al. Alpha-ketoglutarate ameliorates age-related osteoporosis via regulating histone methylations. Nat Commun 2020;11(1):1–14.
[50] Tran TQ, Hanse EA, Habowski AN, Li H, Gabra MBI, Yang Y, et al. α-Ketoglutarate attenuates Wnt signalling and drives differentiation in colorectal cancer. Nat Cancer 2020;1(3):345–58.
[51] Tian Q, Zhao J, Yang Q, Wang B, Deavila JM, Zhu MJ, et al. Dietary alpha-ketoglutarate promotes beige adipogenesis and prevents obesity in middle-aged mice. Aging Cell 2020;19(1):1–10.
[52] Ackermann M, Verladen SE, Kuehnel M, Haverich A, Welte T, Laenger F, et al. Pulmonary vascular endothelialitis, thrombosis and angiogenesis in COVID-19. N Engl J Med 2020;383:120–8.
[53] McMullen PD, Cho JH, Miller JL, Husain AN, Pytel P, Krausz T. A Descriptive and Quantitative Immunohistochemical Study Demonstrating a Spectrum of Platelet Recruitment Patterns Across Pulmonary Infections Including COVID-19. Am J Clin Pathol 2021;155:354–63.
[54] Galluzzi L, Brenner C, Morselli E, Touat Z, Kroemer G. Viral control of mitochondrial apoptosis. PLoS Pathogen 2008;4:e1000018.